Synthesis and Characterization of $K_3Mo_{14}O_{22}$, $K_{1.66}Pb_{1.34}Mo_{14}O_{22}$, and $K_{1.29}Sn_{1.71}Mo_{14}O_{22}$: Oligomeric Clusters with Three Trans Edge-Shared Mo Octahedra

George L. Schimek, S. C. Chen, and Robert E. McCarley*

Ames Laboratory, USDOE, and Department of Chemistry, Iowa State University, Ames, Iowa 50011

Received July 14, 1995[⊗]

The preparation and structural characterization of three new $M_3Mo_{14}O_{22}$ members in the series $M_nMo_{4n+2}O_{6n+4}$ with $n = 3$ have afforded an experimental picture of the relationship between structure and bonding and the number of electrons available for metal−metal bonding. The three compounds, $K_3Mo_{14}O_{22}$, $K_{1.66}Pb_{1.34}Mo_{14}O_{22}$, and $K_{1.29}Sn_{1.71}Mo_{14}O_{22}$, were synthesized from the appropriate quantities of metals, metal oxides, and potassium molybdate fired at 1200-1500 °C for 4−9 days. They were all structured in the space group $P2_1/a$ (No. 14) with $Z = 2$ and $a = 9.916(2)$, 9.917(1), and 9.929(2) Å; $b = 9.325(2)$, 9.276(1), and 9.294(1) Å; $c = 10.439(2)$, 10.3560(9), and 10.338(2) Å; $\beta = 103.96(1)°$, 103.827(7)°, and 104.13(2)°; and R/R_w (%) = 3.14/3.69, 6.00/4.81, and 2.45/2.99; using observed reflections/parameters of 1060/176, 1830/135, and 1015/182, respectively. The materials have condensed clusters with strong metal−metal bonding that are constructed of three trans edge-shared molybdenum octahedra with all edges bridged by oxygen atoms. The important differences among the clusters in these compounds are in the arrangement of the intercluster and apical−apical molybdenum bonding. The trimeric cluster units are interconnected via Mo−O bonding in a stair-step fashion along the c direction. In the $a-b$ plane, Mo−O intercluster bonding creates a pocket in which the cations reside. The changes in bonding are correlated to the increasing number of electrons available for metal−metal bonding, based upon Mo−Mo bond order and Mo−O bond valence sums. Magnetic susceptibility and electrical resistivity results are discussed with respect to the structure and bonding.

Introduction

Compounds with finite chain segments of condensed, trans edge-shared molybdenum octahedra have been fittingly called oligomers.[1] These materials have discrete clusters that are composed of metal−metal bonded Mo octahedra, similar to those observed in the infinite chain compounds, $M_xMo_4O_6$.[2−10] However, various structural distortions abound in the oligomeric members, unlike the $M_xMo_4O_6$ phases. The quest for new materials containing these oligomers is fueled, in part, by the desire to learn more about the relationships that exist between these structural distortions and the number of electrons available for metal−metal bonding (metal cluster electrons, MCE). Promoting the growth of crystalline ternary compounds containing any given oligomer requires an intricate and interdependent set of variables, including reaction temperature and time, transport agents, cationic size, and number of electrons donated to the molybdenum oxide framework by the cations.

Members of the oligomeric series can be represented by the general formulation, $M_nMo_{4n+2}O_{6n+4}$, where n equals the number of trans edge-shared molybdenum octahedra. A brief communication on the first $n = 3$ member, $Tl_{1.6}Sn_{1.2}Mo_{14}O_{22}$, was reported by Simon and co-workers in 1989.[11] A more detailed structural study followed in 1991,[12] and some of its properties are discussed in a recent paper.[13] Three new trimeric ($n = 3$) compounds with electron counts less than that determined for the Tl-Sn member have been synthesized and structurally characterized and some of their magnetic and electrical resistivity properties investigated. These new members are compared and contrasted with $Tl_{1.6}Sn_{1.2}Mo_{14}O_{22}$ via their structural distortions, properties, Mo−Mo bond order, and Mo−O bond valence sums.

Experimental Section

Synthesis. The starting reagents included K_2MoO_4, SnO, Sn, PbO, MoO_3, MoO_2, and Mo. Potassium molybdate was prepared by reacting potassium hydroxide (Fisher Certified ACS) with a stoichiometric quantity of molybdenum trioxide in deionized water. The molybdate solution was filtered, and the white powder was precipitated out from the filtrate by gradually reducing the volume with heating. The wet product was collected on a glass frit and dried at 120 °C overnight. Tin(II) oxide was prepared by the method reported by Weiser and Milligan.[14] Molybdenum dioxide (Alfa, 99%) and lead(II) oxide (Aldrich, 99.9%) were used as commercially obtained. Molybdenum trioxide was fired at 520 °C overnight in an open crucible and then cooled over desiccant. Molybdenum and tin powders (Aldrich, 99.99%, and Fisher, respectively) were dried under dynamic vacuum at 120 °C overnight. All reagents were subsequently stored in a desiccator. In some synthetic work, molybdenum tubing (Thermoelectron Corp., 99.97%) was used as a reaction vessel. The tubing was cleaned by heating at 950 °C for 5 h under a flowing hydrogen atmosphere. After cooling to room temperature under hydrogen, the tubing was also stored over desiccant.

[⊗] Abstract published in *Advance ACS Abstracts,* November 1, 1995.

(1) Mattausch, Hj.; Simon, A.; Peters, E.-M. *Inorg. Chem.* **1986**, *25*, 3428.
(2) Torardi, C. C.; McCarley, R. E. *J. Am. Chem. Soc.* **1979**, *101*, 3963.
(3) Lii, K. H.; Edwards, P. A.; Brough, L. F.; McCarley, R. E. *J. Solid State Chem.* **1985**, *57*, 17.
(4) Torardi, C. C.; McCarley, R. E. *J. Solid State Chem.* **1981**, *37*, 393.
(5) Aufdembrink, B. A. Ph.D. Dissertation, Iowa State University, Ames, IA, 1985.
(6) Torardi, C. C.; McCarley, R. E. *J. Less-Common Met.* **1986**, *116*, 169.
(7) Chen, S. C. Ph.D. Dissertation, Iowa State University, Ames, IA, 1991.
(8) Bauer, K.; Rau, F.; Abriel, W.; Range, K.-J. *Vortragstagung Fachgruppe Festkörperchemie in der GDCh*, Stuttgart, FRG, 1980.
(9) Ramanujachary, K. V.; Greenblatt, M.; Jones, E. B.; McCarroll, W. H. *J. Solid State Chem.* **1993**, *102* (1), 69.
(10) Simon, A. *Angew. Chem., Int. Ed. Engl.* **1988**, *27*, 159.
(11) Dronskowski, R.; Simon, A. *Angew. Chem., Int. Ed. Engl.* **1989**, *28* (5), 758.
(12) Dronskowski, R.; Simon, A. *Acta Chem. Scand.* **1991**, *45*, 850.
(13) Dronskowski, R.; Mattausch, Hj.; Simon, A. *Z. Anorg. Allg. Chem.* **1993**, *619*, 1397.
(14) Weiser, H. Milligan, O. *Inorganic Colloid Chemistry: The Hydrous Oxides and Hydroxides*; Wiley: London, 1933.

0020-1669/95/1334-6130$09.00/0

The crystalline compound, $K_3Mo_{14}O_{22}$, was initially found as a product in a reaction intended to prepare $K_3Mo_{11}O_{17}$ from molybdenum trioxide, molybdenum metal, and a 2-fold excess of potassium molybdate. The excess molybdate salt of potassium (mp 919 °C) was utilized as a molten medium to facilitate the reaction. After firing at 1430 °C for 4 days in an evacuated and sealed molybdenum tube (~2 × 10^{-5} Torr), the mixture was washed with water to remove the unreacted potassium molybdate. However, the crystals from this reaction were small in size, and the structure could not be solved through routine single crystal diffractometer methods.

Larger, good quality crystals of this compound were prepared by reacting a mixture of potassium molybdate, molybdenum dioxide, and molybdenum metal in a mole ratio of 3:11:8 in an evacuated and sealed molybdenum tube fired at 1250 °C for 8 days. Subsequently, a single phase product of $K_3Mo_{14}O_{22}$ was prepared by heating a pressed pellet containing stoichiometric amounts of molybdenum trioxide, molybdenum, and a 2-fold excess of potassium molybdate in an evacuated (~1 × 10^{-4} Torr) and sealed fused silica tube at 1200 °C for 8 days. After having been washed with water to remove the unreacted potassium molybdate, the resulting product was determined to be single phase by Guinier X-ray powder diffraction.

Crystals of $K_{1.66}Pb_{1.34}Mo_{14}O_{22}$ were first discovered in a reaction that was intended to prepare $K_2PbMo_{14}O_{22}$. A pressed pellet with the correct stoichiometry for $K_2PbMo_{14}O_{22}$ was prepared from K_2MoO_4, PbO, MoO_3, and Mo. It was loaded into a molybdenum tube, evacuated, and heated at 400 °C for 2 h under dynamic vacuum before being sealed via electron beam welding. The sample was fired at 1500 °C for 93 h in a vacuum furnace and cooled to 700 °C at 3 °C/min and then furnace cooled. The products of this reaction were black, chunk-like crystals deposited on the upper molybdenum cap and walls, interspersed with beads of lead metal. The remnants of the pellet were a porous matrix of molybdenum metal. Single phase material of $K_{1.66}Pb_{1.34}Mo_{14}O_{22}$ was not prepared since the elemental microprobe analyses on several crystals indicated that the composition was variable.

Crystals of the compound $K_{1.29}Sn_{1.71}Mo_{14}O_{22}$ were first discovered as a product in a reaction that was intended to prepare the quaternary $K_2Sn_2Mo_{18}O_{28}$, an $n = 4$ oligomer in the $M_nMo_{4n+2}O_{6n+4}$ series. A pressed pellet with the correct stoichiometric ratio of K_2MoO_4, SnO, MoO_2, and Mo for the tetrameric oligomer was loaded into a molybdenum tube and sealed under vacuum by electron beam welding. The sample was fired at 1500 °C for 94 h in a vacuum furnace and cooled to 1200 °C over 3 h, to 800 °C over 1 h, and then furnace cooled. Upon opening the tube, numerous black crystals with chunk-like morphology were found on the upper molybdenum cap, along with silvery beads of tin metal. The upper tube walls also contained a multitude of crystals, all of which had well-defined faces. All that remained of the pellet was a porous matrix of molybdenum metal. The composition of the black, chunk-like crystals was determined through a single crystal structure refinement. Preparation of single phase $K_{1.29}Sn_{1.71}Mo_{14}O_{22}$ was undertaken. A loose powder containing an intimate mixture of K_2MoO_4, Sn, MoO_3, and Mo in the proper mole ratio was loaded into a fused silica tube with a 1-fold excess of K_2MoO_4. The system was evacuated and heated to 300 °C for 1 h to remove adventitious water. The reaction tube was then sealed and loaded into an outer fused silica tube, which was subsequently evacuated before being sealed. This outer jacket was utilized to prevent the oxidation of the sample by air if the inner fused silica tube were to fail, due to its reaction with the potassium molybdate. The sample was fired at 1250 °C for 9 days. After firing, the inner tube was found to be badly devitrified, but the contents appeared to be unaffected, and the outer fused silica jacket was intact. The product contained the same chunk-like crystals, as described above, embedded in a loose black powder. Also, a few needles of molybdenum dioxide were found transported to the tube walls. A Guinier X-ray powder pattern of a mixture of bulk powder and crystals indicated the presence of only an $n = 3$ oligomer. The degradation of the fused silica tube indicated that the excess molybdate reacted with the container. Reactions utilizing a stoichiometric quantity of potassium molybdate were also tested and resulted in the formation of the correct oligomer; however, a significant amount of tin metal always remained. Microprobe analyses indicated that the potassium and tin content in this oligomeric member were variable.

Elemental Microprobe Analyses. Quantitative elemental analyses were completed on the K-Pb and K-Sn oligomeric members with an ARL SEMQ microprobe. The instrument was equipped with wavelength dispersive spectrometers and operated at 15 kV and 25 nA. All samples were mounted in Epo-Tek 301-2 epoxy resin, dried, and polished to produce a flat surface. Prior to examination, the samples were sputtered with carbon to ensure conductivity. Peak profiles and backgrounds were measured for standards immediately before the analyses.

The selected K-Pb crystals were taken from the same reaction product as the crystal for X-ray data collection. The results indicated a wide compositional variation. Approximately 26 different grains were analyzed for K, Pb, and Mo. Oxygen was calculated by difference and always resulted in values near the expected 22/formula unit. Three distinct compositions were observed. One set of 20 data points gave an average composition of $K_{1.99(7)}Pb_{1.00(7)}Mo_{14}O_{22}$, another set of 29 points averaged to $K_{1.55(3)}Pb_{1.45(5)}Mo_{14}O_{22}$, and a third set containing 16 data points averaged to $K_{1.74(4)}Pb_{1.26(5)}Mo_{14}O_{22}$. The composition determined by the single crystal refinement clearly falls within the scope of the results calculated from microprobe analyses. The results verify that all the cation pockets are fully occupied since the cation to Mo ratios were nearly 3:14.

Microprobe analyses were also completed on crystals taken from the original reaction of the K-Sn member where the K:Sn mole ratio was prepared to be 1. Again, K, Sn, and Mo were analyzed and oxygen was calculated by difference. The analyses of two crystals, with seven data points each, indicated the average K:Sn mole ratios were 0.83 and 0.86, respectively. These values are significantly higher than the 0.75 mole ratio determined by the single crystal refinement. Since analyses of various other crystals of the K-Sn oligomer gave inconsistent results, the single crystal that was used for data collection was mounted for microprobe analyses. The results from this analysis were more fruitful. Five data points gave an average K:Sn mole ratio of 0.77 (or a molar composition of $K_{1.31(2)}Sn_{1.71(5)}Mo_{14}O_{22}$). This value was in good agreement with the single crystal refinement.

X-ray Single Crystal Studies. All crystals were mounted on glass fibers with quick-drying epoxy resin and studied with a Rigaku AFC6R rotating anode diffractometer, equipped with graphite monochromated Mo Kα radiation (λ = 0.71069 Å) generated at 7 kW. An $\omega - 2\theta$ scan mode was utilized. All three data sets were collected at 23 °C, and three standard reflections were measured every 150 reflections and showed no apparent variation in intensity during the data collections. The intensity data were corrected for Lorentz and polarization effects.

A black, trigonal prismatic crystal of $K_3Mo_{14}O_{22}$ having the dimensions 0.06 × 0.06 × 0.08 mm^3 was utilized. Although such a small crystal definitely limited the number of observed reflections, all larger crystals examined were badly affected by twinning. Lattice parameters and an orientation matrix for data collection were derived from 15 randomly located and centered reflections with a 2θ range of 13−17°. The lattice was found to belong to the monoclinic system with cell dimensions of a = 9.916(2) Å, b = 9.325(2) Å, c = 10.439(2) Å, β = 103.96(1)°, and vol = 936.7(5) $Å^3$. Data were collected from 0° to 50° in 2θ in the octants $(h,k,\pm l)$. The number of reflections measured was 1878, of which 1771 were unique and 1060 were observed with $I > 3\sigma(I)$. The linear absorption coefficient for Mo Kα radiation was 96.97 cm^{-1}. An empirical absorption correction[15] was applied, based upon an azimuthal scan of a reflection with a transmission range of 0.873−1.000.

A black crystal of $K_{1.66}Pb_{1.34}Mo_{14}O_{22}$ measuring 0.15 × 0.20 × 0.28 mm^3 was mounted. Lattice parameters and an orientation matrix for data collection were derived from 14 randomly located and centered reflections with a 2θ range of 13−16°. A subsequent refinement on 25 reflections with strong intensities and 2θ values ranging from 39° to 41° gave a final cell with monoclinic lattice parameters of a = 9.917(1) Å, b = 9.276(1) Å, c = 10.3560(9) Å, β = 103.827(7)°, and vol = 925.1(2) $Å^3$. Data were collected from 0° to 55° in 2θ in the octants $(h,k,\pm l)$. The linear absorption coefficient for Mo Kα radiation was 229.19 cm^{-1}. The number of reflections measured was 2403, of which 2009 were unique and 1830 were observed with $I > 3\sigma(I)$.

(15) North, A. C. T.; Phillips, D. C.; Mathews, F. S. *Acta Crystallogr.* **1968**, *A24*, 351.

Because of the very complex faceting of the crystal, an analytical absorption correction could not be applied. Thus, a θ-dependent spherical absorption correction[16] was applied based upon an average radius of 0.1 mm and three azimuthal scans of reflections with a transmission range of 0.563−1.000.

Again twinning effects in larger crystals of $K_{1.29}Sn_{1.71}Mo_{14}O_{22}$ made it necessary to choose a small crystal. Thus, a black, chunk-like crystal measuring 0.06 × 0.08 × 0.10 mm^3 was utilized for data collection. Lattice parameters and an orientation matrix for data collection were derived from 22 randomly located and centered reflections with a 2θ range of 12−17°. A subsequent refinement on 25 reflections with strong intensities and 2θ values near 40° gave a final cell with monoclinic lattice parameters of a = 9.929(2) Å, b = 9.294(1) Å, c = 10.338(2) Å, β = 104.13(2)°, and vol = 925.1(3) Å^3. Oscillation photographs about the three crystallographic axes showed no reflections indicative of any superstructuring. Data were collected from 0° to 50° in 2θ in the hemisphere (h,±k,±l). The number of reflections measured was 3417, of which 2066 were unique (R_{int} = 0.044) and 1015 were observed with $I > 3\sigma(I)$. The linear absorption coefficient for Mo Kα radiation was 115.17 cm^{-1}. An empirical absorption correction[15] was applied, based upon one azimuthal scan of a reflection with a transmission range of 0.763−1.000.

Structure Solutions and Refinements. The space group $P2_1/a$ (No. 14) was chosen for $K_3Mo_{14}O_{22}$ based on the systematic absences of $h0l$: $h \neq 2n$ and $0k0$: $k \neq 2n$. The structure was solved by direct methods, MULTAN,[17] and refined on $|F|$ by full matrix, least squares techniques[18] in the TEXSAN[19] package. All but three oxygen atoms (O4, O10, and O11) could be refined anisotropically to give R = 5.2% and R_w = 6.8%. A θ-dependent numerical correction for absorption was then applied and the structure refined with the CHES programs.[16] The subsequent structure was refined with all atomic thermal parameters anisotropic and converged at R = 3.4% and R_w = 4.1%. At this stage, the temperature factors of the oxygen atoms were highly anisotropic. A secondary extinction correction was applied and refined to 2.946(1) × 10^{-6}. The temperature factors of the oxygen atoms improved, and the refinement converged at R = 0.0314 and R_w = 0.0369 with a maximum shift in the final cycle of 0.005 for 176 variables over 1060 observed reflections. The final electron density difference map was flat, with the largest peak of +2.0 e/Å^3 near Mo3.

The space group $P2_1/a$ (No. 14) was also chosen for $K_{1.66}Pb_{1.34}Mo_{14}O_{22}$ based upon the systematic absences of $h0l$: $h \neq 2n$ and $0k0$: $k \neq 2n$. However, there were 15 violations of the former condition and one violation of the latter. Some, although not all, of the violations were found to be spatially close to very intense reflections. Therefore, the data were processed in three space groups: $P2_1$, Pa, and $P2_1/a$; and the predicted refinement based on SHELXS[20] direct methods was 0.022, 0.027, and 0.032, respectively. The structure was subsequently solved in $P2_1$ and $P2_1/a$.

The refinement in $P2_1$ converged at R = 5.58% and R_w = 7.49%; however, only the thermal parameters of the heavy atoms would refine isotropically, and the oxygen atom thermal parameters could not be varied. This solution was not data limited (13:1 data to parameter ratio) even though all atoms become unique in $P2_1$. The general structural features were essentially identical to the refinement in $P2_1/a$, with only small distortions.

The structure was therefore solved in $P2_1/a$ by direct methods using SHELXS[20] and refined on $|F|$ by full matrix, least squares techniques[18] with the TEXSAN[19] package. The lattice parameters and systematic absences indicated that this phase also should be isostructural to $K_3Mo_{14}O_{22}$. Therefore, atomic positions for the molybdenum and oxygen atoms were entered based upon the $K_3Mo_{14}O_{22}$ member. A refinement on these positional parameters converged at 31%. The two major cation positions were then easily located from a Fourier difference map. With these two cation positions refined, their occupancies were varied with a combination of potassium and lead using a fixed B_{eq}, whereupon the R factor decreased to 13%. Appropriate variation of isotropic thermal parameters converged at R = 7.9% and R_w = 10%. Subsequently, a DIFABS[21] correction was also applied to the isotropically refined data. This step was deemed necessary since the absorption correction still did not appear to provide an adequate correction. Now all the heavy atom and two oxygen atom thermal parameters could be refined anisotropically, and the remaining nine oxygen atom temperature factors were treated isotropically. Because microprobe analyses indicated that the cation:Mo ratio was 3:14, potassium and lead were allowed to refine on both sites, with the only restriction being full occupancy. This set of conditions converged at R = 6.00% and R_w = 4.81%, with the origin refined as 76.0(6)% K and 24.0(6)% Pb and the second unique cation position refined as 45.0(8)% K and 55.0(8)% Pb. The final formulation for this compound was $K_{1.66(1)}Pb_{1.34(1)}Mo_{14}O_{22}$. The final cycle utilized 135 variables over 1830 reflections and had a maximum shift of 0.01. The final electron difference map indicated that the largest peak of +4.53 e/Å^3 was located 1.63 Å from Pb2 and 2.09 Å from O8 and the smallest peak of −4.11 e/Å^3 was located 0.80 Å from Pb2. Since this phase contains a significant quantity of lead, the absorption correction applied may still have been poor. Second, the relatively large residual electron density has become typical of oligomeric members whose "single" crystals actually contain defects in the form of intergrowth of oligomers with different values of n and/or different modes of cluster interconnections.[13,22]

The space group $P2_1/a$ (No. 14) also was chosen for $K_{1.29}Sn_{1.71}Mo_{14}O_{22}$, based upon the systematic absences of $h0l$: $h \neq 2n$ and $0k0$: $k \neq 2n$. The structure was solved by direct methods using SHELXS[20] (R = 0.037) and refined on $|F|$ by full matrix, least squares techniques[18] with the TEXSAN[19] package. Based upon the lattice parameters and systematic absences, the molybdenum oxide framework was presumed to be isostructural to $K_3Mo_{14}O_{22}$. Therefore, atomic positions for the molybdenum and oxygen atoms were entered based upon the $K_3Mo_{14}O_{22}$ member. These parameters converged at R = 24%. Two cation positions were located from electron density difference maps, one at the origin and one at approximately 0,0,0.35. These two positions were entered as K1 and Sn2, respectively, based upon the quantity of electron density at those positions. With these atoms included, the refinement converged at 17%. All the atomic thermal parameters were then refined isotropically. Cation occupancies were allowed to vary, with the M1 site containing potassium and/or tin, but the M2 site occupancy was only refined with tin. These cation choices were based upon acceptable cation−oxygen bond distances (K and/or Sn) and compared to those calculated in this phase. All molybdenum atom thermal parameters were then refined anisotropically. The refinement converged at R = 5.9%. At this point, a Fourier difference map revealed two more cation sites, one located near the origin (~0.5 Å away) and the second about 0.7 Å from the cation at the general position. Neither peak was accounted for by the thermal parameters of the cations already refined. Both peaks were entered, Sn1A and K2A, and positionally refined with very low occupancies, to prevent the refinement from diverging. After convergence, the satellite position near the origin and its occupancy were refined solely as tin, due to two short cation−oxygen bond distances that could not reasonably be accepted as potassium−oxygen distances, and the position at the origin was refined with only potassium. Together, the origin and its satellite were determined to be fully occupied, and both of their thermal parameters were refined anisotropically. The satellite related to Sn2 was refined as potassium. Based upon bond valence sums, potassium or tin could occupy the satellite position; however, microprobe analyses indicated that no more tin should be present, and therefore, potassium was chosen to reside in this site. This second cation and its satellite also refined to full occupancy. In this case, the thermal parameter of the major site, Sn2, was refined anisotropically, however, the corresponding thermal

(16) Jacobson, R. A. CHES: Single crystal x-ray data preparation and structure refinement programs, Iowa State University/Ames Lab, Ames, IA, 50011.
(17) Main, P.; Friske, S. J.; Hull, S. E.; Lessinger, L.; Germain, G.; Declercq, J.-P.; Woolfson, M. M. MULTAN 80. A System of Computer Programs for the Automatic Solution of Crystal Structures from X-ray Diffraction Data, University of York, York, England, 1980.
(18) Busing, W. R.; Martin. K. O.; Levy, H. A. ORFLS, A FORTRAN Crystallographic Least Squares Program, Report ORNL-TM-305, Oak Ridge National Laboratory, Oak Ridge, TN, 1962.
(19) TEXSAN: Single Crystal Structure Analysis Software, Version 5.0, 1989. Molecular Structure Corp., The Woodlands, TX 77381.
(20) Sheldrick, G. M. *Crystallographic Computing 3*, Oxford University Press, 1985.
(21) Walker, N.; Stuart, D. *Acta Crystallogr.* **1983**, *A39*, 1558.
(22) Schimek, G. L.; Nagaki, D.; McCarley, R. E. *Inorg. Chem.* **1994**, *33*, 1259.

Table 1. X-ray Crystallographic Data for the Trimeric Oligomers[a]

formula	$K_3Mo_{14}O_{22}$	$K_{1.66}Pb_{1.34}Mo_{14}O_{22}$	$K_{1.29}Sn_{1.71}Mo_{14}O_{22}$
formula wt	1812.46	2037.70	1948.54
crystal system	monoclinic	monoclinic	monoclinic
space group	$P2_1/a$ (No. 14)	$P2_1/a$ (No. 14)	$P2_1/a$ (No. 14)
a, Å	9.916(2)	9.917(1)	9.929(2)
b, Å	9.325(2)	9.276(1)	9.294(1)
c, Å	10.439(2)	10.3560(9)	10.338(2)
β, deg	103.96(1)	103.827(7)	104.13(2)
vol, Å^3	936.7(5)	925.1(2)	925.1(3)
Z	2	2	2
calcd density, g/cm^3	6.425	7.313	6.975
μ, cm^{-1}	96.97	229.19	115.17
R^b, R_w^c	0.0314, 0.0369	0.0600, 0.0481	0.0245, 0.0299

[a] All data collected with Mo Kα radiation, $\lambda = 0.71069$ Å. [b] $R = \sum||F_o| - |F_c||/\sum|F_o|$. [c] $R_w = [\sum w\{|F_o| - |F_c|\}^2/\sum w|F_o|^2]^{1/2}$; $w = 1/\sigma^2\{|F_o|\}$.

Table 2. Atomic Coordinates for $K_3Mo_{14}O_{22}$

atom[a]	X	Y	Z	B_{eq}[b]
K1	0.0	0.0	0.0	1.6(1)
K2	0.0667(3)	0.0119(4)	0.3136(3)	1.6(1)
Mo1	0.1227(1)	0.3885(1)	0.1400(1)	0.98(5)
Mo2	0.9146(1)	0.3774(1)	0.2748(1)	0.99(5)
Mo3	0.2282(1)	0.6263(1)	0.2876(1)	1.03(5)
Mo4	0.8473(1)	0.3706(1)	0.0144(1)	1.02(5)
Mo5	0.1906(1)	0.3843(1)	0.4104(1)	1.04(5)
Mo6	0.0474(1)	0.3814(1)	0.8647(1)	1.04(5)
Mo7	0.9754(1)	0.3719(1)	0.5934(1)	1.00(5)
O1	0.3254(12)	0.7596(12)	0.9945(9)	1.5(6)
O2	0.4017(10)	0.7559(11)	0.2812(8)	1.1(5)
O3	0.3143(12)	0.2555(10)	0.5722(8)	1.3(5)
O4	0.1430(10)	0.5049(11)	0.5630(8)	1.0(4)
O5	0.2235(10)	0.5011(11)	0.8571(8)	1.0(4)
O6	0.7154(10)	0.4799(10)	0.8580(9)	1.0(4)
O7	0.3864(13)	0.2511(10)	0.8593(10)	1.2(4)
O8	0.6527(10)	0.4899(11)	0.5753(9)	1.2(4)
O9	0.9694(11)	0.7323(11)	0.5627(9)	1.1(4)
O10	0.2536(11)	0.7580(10)	0.7128(8)	1.0(4)
O11	0.9694(12)	0.2373(10)	0.1502(9)	1.0(4)

[a] All atoms reside on the Wyckoff position 4e, except K1, which resides on 2a. [b] The equivalent isotropic temperature factor, B_{eq}, is defined as $8\pi^2/3\ \{\sum_i\sum_j(U_{ij}a^*_i a^*_j\bar{a}_i\cdot\bar{a}_j)\}$, where the summations of i and j range from 1 to 3.

parameters for the potassium satellite, K2A, would only refine isotropically. This thermal behavior was most likely due to the proximity of the large electron density from the majority site, Sn2. The thermal parameters for the oxygen atoms that could be refined anisotropically, without becoming nonpositive definite, were varied. When a secondary extinction correction was applied and refined to $3.1(2) \times 10^{-7}$, the residual decreased to $R = 2.45\%$. This correction improved the overall thermal behavior of the oxygen atoms and consequently allowed three more oxygen atoms to be refined anisotropically.

The final occupancy for the potassium at the origin was determined to be 59(1)%. The satellite tin atom, Sn1A, had an occupancy of 41(1)%. Sn2 was refined with an occupancy of 64.8(6)% with the satellite, K2A, at 35.2(6)% occupancy. This cation assessment results in the following formulation, $K_{1.29(1)}Sn_{1.71(1)}Mo_{14}O_{22}$, in good agreement with microprobe analyses. The final refinement converged at $R = 0.0245$ and $R_w = 0.0299$ with anisotropic refinement of all seven molybdenum atoms, nine of the eleven oxygen atoms, and three of the four unique cations. The final cycle refined 182 variables over 1015 reflections and had a maximum shift of 0.099. A final Fourier electron difference map indicated that the largest peak of +1.07 e/Å^3 was located 1.4 Å from Mo4 and the smallest peak of −1.09 e/Å^3 was located 1.7 Å from Mo4 and 2.3 Å from Mo6.

A summary of the data collection and refinement for all three trimeric oligomers is given in Table 1. Final positional and isotropic temperature parameters are found in Tables 2−4.

Magnetic Susceptibility. The magnetic properties of $K_3Mo_{14}O_{22}$ were examined on a powdered sample loaded in a quartz tube. Selected crystals of the K-Pb and K-Sn members were also loaded into quartz tubing for measurement. Data were obtained on a Quantum Design SQUID magnetosusceptometer. The experimental data were subsequently corrected for the diamagnetic contribution from the quartz.

Electrical Resistivity. The temperature-dependent electrical resistivity of $K_3Mo_{14}O_{22}$ was measured on a pressed pellet which had been sintered in an evacuated fused silica ampoule at 1200 °C for 1 day after the initial synthesis. The measurement was based on the van der Pauw four-probe method for electrical conductivity.[23] The sample was prepared by attaching four platinum wires, which served as the voltage and current leads, to the pellet with Epo-Tech silver epoxy. The voltage drops across the sample were recorded as a function of temperature.

Table 3. Atomic Coordinates for $K_{1.66}Pb_{1.34}Mo_{14}O_{22}$

atom[a]	X	Y	Z	B_{eq}[b]
K1/Pb1[c]	0.0	0.0	0.0	2.0(2)
K2/Pb2[d]	0.0552(2)	0.0099(2)	0.3349(1)	1.50(6)
Mo1	0.1213(2)	0.3876(2)	0.1391(2)	0.31(5)
Mo2	0.9108(2)	0.3763(2)	0.2735(2)	0.40(6)
Mo3	0.2261(2)	0.6305(2)	0.2888(1)	0.38(6)
Mo4	0.8466(2)	0.3706(2)	0.0116(2)	0.40(6)
Mo5	0.1892(2)	0.3837(2)	0.4123(1)	0.33(6)
Mo6	0.0483(2)	0.3794(2)	0.8601(1)	0.32(6)
Mo7	0.9774(2)	0.3841(2)	0.5818(2)	0.47(6)
O1	0.174(1)	0.245(1)	0.003(1)	0.3(2)
O2	0.402(1)	0.755(1)	0.287(1)	0.5(2)
O3	0.185(1)	0.744(1)	0.428(1)	0.4(2)
O4	0.845(1)	0.495(1)	0.423(1)	0.3(2)
O5	0.776(1)	0.499(1)	0.139(1)	0.5(2)
O6	0.287(1)	0.519(1)	0.146(1)	0.5(2)
O7	0.113(1)	0.743(1)	0.143(1)	0.4(2)
O8	0.349(1)	0.507(2)	0.424(1)	0.6(2)
O9	0.029(2)	0.260(1)	0.431(1)	0.8(2)
O10	0.257(2)	0.243(2)	0.285(1)	0.9(5)
O11	0.970(2)	0.236(1)	0.147(1)	0.7(5)

[a] All atoms reside on the Wyckoff position 4e, except K1/Pb1, which resides on 2a. [b] The equivalent isotropic temperature factor, B_{eq}, is defined as $8\pi^2/3\ \{\sum_i\sum_j(U_{ij}a^*_i a^*_j\bar{a}_i\cdot\bar{a}_j)\}$, where the summations of i and j range from 1 to 3. [c] K1 and Pb1 have occupancies of 76.0(6)% and 24.0(6)%, respectively. [d] K2 and Pb2 have occupancies of 45.0(8)% and 55.0(8)%, respectively.

Table 4. Atomic Coordinates for $K_{1.29}Sn_{1.71}Mo_{14}O_{22}$

atom[a]	X	Y	Z	B_{eq}[b]
K1[c]	0.0	0.0	0.0	3.(1)
Sn1A[c]	0.036(2)	0.990(3)	0.039(2)	3.0(5)
Sn2[d]	0.0449(1)	0.0281(1)	0.3528(1)	1.30(5)
K2A[d]	0.0633(9)	0.005(1)	0.2994(9)	1.6(2)
Mo1	0.11946(8)	0.3850(1)	0.13931(8)	0.40(3)
Mo2	0.91251(8)	0.3799(1)	0.28156(9)	0.61(3)
Mo3	0.22609(9)	0.6317(1)	0.2828(1)	0.73(4)
Mo4	0.84360(9)	0.3717(1)	0.0004(1)	0.92(4)
Mo5	0.19152(9)	0.3842(1)	0.41321(8)	0.42(3)
Mo6	0.05033(8)	0.3819(1)	0.86318(8)	0.46(3)
Mo7	0.9750(1)	0.3783(1)	0.5831(1)	0.85(4)
O1	0.1733(7)	0.2576(8)	0.0033(7)	0.7(3)
O2	0.4004(7)	0.7579(8)	0.2844(6)	0.6(3)
O3	0.1839(7)	0.7544(8)	0.4295(6)	0.8(3)
O4	0.8486(7)	0.4994(9)	0.4286(7)	1.1(1)
O5	0.7794(7)	0.4926(8)	0.1398(6)	0.9(3)
O6	0.2889(7)	0.5105(8)	0.1441(6)	0.9(1)
O7	0.1079(8)	0.7600(8)	0.1425(7)	1.0(3)
O8	0.3553(6)	0.5066(7)	0.4255(7)	0.6(2)
O9	0.0309(7)	0.2564(8)	0.4299(7)	0.8(3)
O10	0.2432(7)	0.2555(7)	0.2879(6)	0.8(3)
O11	0.9620(8)	0.2432(8)	0.1462(7)	1.0(3)

[a] All atoms reside on the Wyckoff position 4e, except K1, which resides on 2a. [b] The equivalent isotropic temperature factor, B_{eq}, is defined as $8\pi^2/3\ \{\sum_i\sum_j(U_{ij}a^*_i a^*_j\bar{a}_i\cdot\bar{a}_j)\}$, where the summations of i and j range from 1 to 3. [c] Sn1A is a satellite of K1, with occupancies of 41(1)% and 59(1)%, respectively. [d] Sn2 has an occupancy of 64.8(6)% with a satellite labeled K2A that has an occupancy of 35.2(6)%.

(23) van der Pauw, L. J. *Philips Res. Rep.* **1958**, *13*, 1.

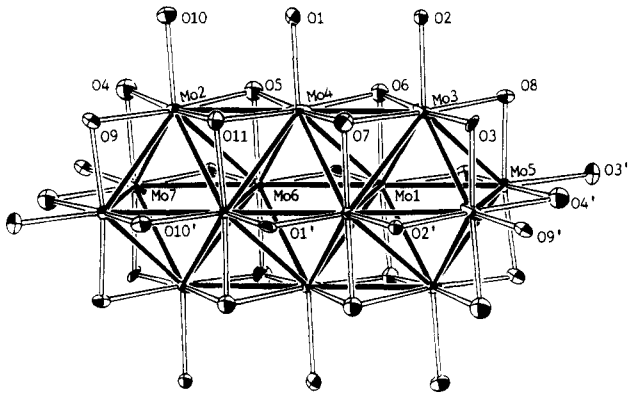

Figure 1. An ORTEP representation (70% thermal ellipsoids) of the $Mo_{14}O_{34}$ cluster observed in $K_{1.29}Sn_{1.71}Mo_{14}O_{22}$. Note the four nearly equivalent apical–apical Mo bond distances, Mo_2–Mo_4 and Mo_3–Mo_4.

The temperature readings were provided by platinum and carbon glass resistance thermometers. The voltage across a standard calibrated resistor was measured periodically to ensure a constant current throughout the experiment.

Results and Discussion

It is now realized that $K_3Mo_{14}O_{22}$ is the same compound reported as $K_2Mo_{12}O_{19}$ in a preliminary publication in 1981.[4] The earlier formulation was based solely upon analytical data and a chemical oxidation state determination. Translation of the earlier formula to a basis with 14 Mo atoms gives the new formula of $K_{2.33}Mo_{14}O_{22.2}$, not far from the actual composition now established by the X-ray structure determination.

Description of Structure. $K_3Mo_{14}O_{22}$, $K_{1.66}Pb_{1.34}Mo_{14}O_{22}$, and $K_{1.29}Sn_{1.71}Mo_{14}O_{22}$ all have a molybdenum oxide cluster framework built from the condensation of three Mo_6O_{18} units along trans edges. All exterior edges of the metal–metal bonded octahedra in the trimeric clusters are bridged by oxygen atoms. The waist Mo atoms at the ends of the cluster and also the apical Mo atoms have terminal bonds to oxygen. Figure 1 shows an ORTEP[24] representation of the configuration observed for the $Mo_{14}O_{34}$ cluster, the basic building block of these compounds. In the K and K-Pb members the apical molybdenum atom bond distances alternate in a short–long manner. The apical molybdenum atoms move together in a pairwise fashion to create strong Mo–Mo bonds (Mo2–Mo4: 2.639(2) Å and 2.634(2) Å for the K and K-Pb members, respectively) and also an essentially nonbonded apical Mo–Mo interaction (Mo3–Mo4: 3.060(2) Å and 3.021(2) Å for the K and K-Pb members, respectively). However, in the K-Sn member (Figure 1) the apical Mo–Mo bond distances are nearly equivalent (Mo2–Mo4, 2.820(1) Å, and Mo3–Mo4, 2.839(1) Å), like those observed in $Tl_{1.6}Sn_{1.2}Mo_{14}O_{22}$.[12] Thus the apical–apical interactions found in the clusters of $K_3Mo_{14}O_{22}$ and $K_{1.66}Pb_{1.34}Mo_{14}O_{22}$ reflect a different electronic configuration than that reported in $Tl_{1.6}Sn_{1.2}Mo_{14}O_{22}$. An ORTEP representation of the cluster displaying its bonding to neighboring clusters in the same chain is shown in Figure 2. All three compounds have the same type of interconnections, but they also show important differences in the degree of intercluster bonding, with Mo7–Mo7′ distances of 3.194(2) Å, 2.838(4) Å, and 2.955(2) Å for the K, K-Pb, and K-Sn members, respectively. Thus, between the varying degrees of apical–apical and intercluster interactions, these three materials all show different modes of bonding to utilize the electrons available for metal–metal bonding.

The angular relationships of the waist molybdenum atoms in $K_3Mo_{14}O_{22}$, $K_{1.66}Pb_{1.34}Mo_{14}O_{22}$, and $K_{1.29}Sn_{1.71}Mo_{14}O_{22}$ agree quite well with the ideal Mo_6 octahedron. The interior bond angles in the basal planes average 90.0 ± 0.9°, 90.0 ± 0.7°, and 90.1 ± 0.6°, respectively. The bond angles between adjacent Mo_6 octahedra along the basal edges parallel to the chain direction are nearly linear for the K, K-Pb, and K-Sn members (177.47(6)°, 177.59(9)°, and 178.93(5)° for Mo5–Mo1–Mo6 and 179.35(6)°, 177.54(9)°, and 178.94(4)° for Mo1–Mo6–Mo7, respectively). Thus, the strong pairwise Mo–Mo bonding seen between the apical molybdenum atoms

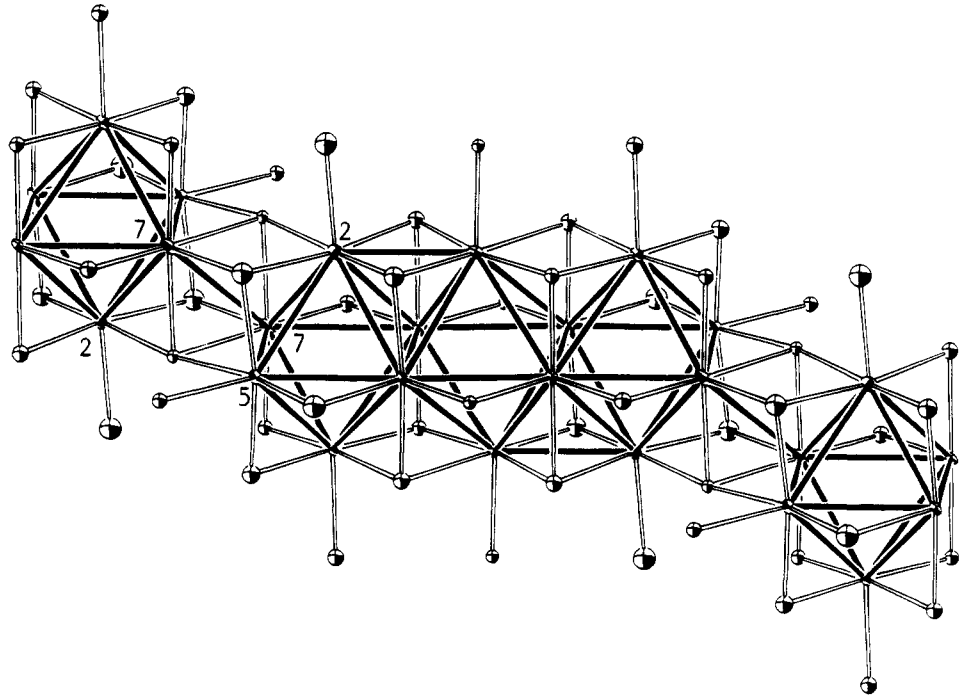

Figure 2. A view perpendicular to the *c* axis of $K_3Mo_{14}O_{22}$ or $K_{1.66}Pb_{1.34}Mo_{14}O_{22}$ showing the short–long arrangement of apical–apical Mo–Mo bonds within one cluster unit, and fragments of neighboring clusters included to indicate the stair-step manner in which the oligomeric units interconnect. The Mo7–Mo7′ intercluster bond is not present in $K_3Mo_{14}O_{22}$. Figure drawn with 70% thermal ellipsoids.

Table 5. Selected Metal–Metal Interatomic Distances (Å) for the Trimeric Oligomers[a]

	$K_3Mo_{14}O_{22}$	$K_{1.66}Pb_{1.34}Mo_{14}O_{22}$	$K_{1.29}Sn_{1.71}Mo_{14}O_{22}$
Mo1–Mo2′	2.765(2)	2.774(2)	2.804(1)
Mo1–Mo3	2.758(2)	2.792(2)	2.795(1)
Mo1–Mo4	2.822(2)	2.794(2)	2.767(1)
Mo1–Mo4′	2.735(2)	2.734(2)	2.755(1)
Mo1–Mo5	2.739(2)	2.748(2)	2.746(1)
Mo1–Mo6	2.791(2)	2.806(2)	2.768(1)
Mo1–Mo6′	2.722(2)	2.740(2)	2.741(1)
Mo2–Mo4 apical[b]	2.639(2)	2.634(2)	2.820(1)
Mo2–Mo5′	2.761(2)	2.793(2)	2.773(1)
Mo2–Mo6	2.754(2)	2.735(2)	2.747(1)
Mo2–Mo7	2.797(2)	2.761(2)	2.736(1)
Mo2–Mo7′ inter[c]	3.234(2)	3.103(2)	3.026(1)
Mo3–Mo4 apical	3.060(2)	3.021(2)	2.839(1)
Mo3–Mo5	2.666(2)	2.689(2)	2.730(1)
Mo3–Mo6′	2.811(2)	2.790(3)	2.794(1)
Mo3–Mo7′	2.613(2)	2.680(2)	2.696(1)
Mo4–Mo6	2.720(2)	2.750(2)	2.759(1)
Mo4–Mo6′	2.808(2)	2.823(2)	2.767(1)
Mo5–Mo7′	2.801(2)	2.725(2)	2.764(1)
Mo5–Mo7′ inter	3.191(2)	3.042(2)	3.091(1)
Mo6–Mo7	2.750(2)	2.800(2)	2.808(1)
Mo7–Mo7′ inter	3.194(2)	2.838(4)	2.955(2)
Sn2···K2A[d]	na[e]	na	0.660(8)
M2···M2[d,f] inter	4.408(3)	3.836(3)	3.414(3)
Sn2···Sn1A[d]	na	na	3.303(8)
K2A···Sn1A[d]	na	na	2.70(1)
K2A···K1[d,f]	3.181(3)	3.380(1)	3.004(9)
Sn1A···Sn1A′[d]	na	na	0.93(2)
Sn1A···K1[d]	na	na	0.464(9)

[a] Atoms with primed numbers are related to those with unprimed numbers by the inversion center. [b] Apical–apical Mo–Mo bond distances. [c] Intercluster Mo–Mo bond distances. [d] Partially occupied positions for K-Pb or K-Sn members. [e] na = not applicable. [f] M2 = K2 in $K_3Mo_{14}O_{22}$, Pb2 in $K_{1.66}Pb_{1.34}Mo_{14}O_{22}$, and Sn2 in $K_{1.29}Sn_{1.71}Mo_{14}O_{22}$. K2A is simply K2 in $K_3Mo_{14}O_{22}$ and $K_{1.66}Pb_{1.34}Mo_{14}O_{22}$.

in the K and K-Pb trimers is the result of a sliding motion of the apical Mo atoms,[22] and not a tilting interaction. In $K_3Mo_{14}O_{22}$ the trans edge-shared molybdenum bond distances perpendicular to the chain direction differ among themselves by about 0.08 Å, with Mo5–Mo7 at 2.801(2) Å at the two ends of the trimer and Mo1–Mo6′ at 2.722(2) Å at the center. However, these shared edges in $K_{1.66}Pb_{1.34}Mo_{14}O_{22}$ and $K_{1.29}Sn_{1.71}Mo_{14}O_{22}$ are nearly equidistant, with Mo5–Mo7′ at 2.725(2) Å and 2.764(1) Å and Mo1–Mo6′ at 2.740(2) Å and 2.741(1) Å, respectively. This relationship also supports the view of a condensation of three nearly regular octahedra along trans edges and is likewise reflected in the nearly equivalent apical Mo–Mo bond distances of the K-Sn member. A complete list of metal–metal bond distances is given in Table 5.

The average intracluster metal–metal bond distance is 2.764 Å for $K_3Mo_{14}O_{22}$, 2.768 Å for $K_{1.66}Pb_{1.34}Mo_{14}O_{22}$, and 2.769 Å for $K_{1.29}Sn_{1.71}Mo_{14}O_{22}$, which all correlate well with the 2.78 Å reported for $Tl_{1.6}Sn_{1.2}Mo_{14}O_{22}$.[12] This similarity is rather striking in view of the differences in the metal–metal bonding. However, a more accurate measure of the utilization of electrons available for metal–metal bonding is through bond order sums,[25] which will be discussed later. Excluding the apical–apical Mo bonds, the shortest metal–metal bond distance in all of the $n = 3$ oligomers is the Mo3–Mo7′ distance, an exterior edge of the outer octahedron. We note that this may arise from a combination of two different structural effects. First, the apical–apical bonding between Mo2 and Mo4 releases Mo3 for greater interaction with its neighbors, Mo5 and Mo7′.

(24) Johnson, C. K. *ORTEP-II, A FORTRAN Thermal-Ellipsoid Plot Program*, Report ORNL-5138, Oak Ridge National Laboratory, Oak Ridge, TN, 1976.
(25) McCarley, R. E. *Polyhedron* **1986**, *5*, 51.

Table 6. Selected Metal–Oxygen Bond Distances (Å) for the Trimeric Oligomers[a]

	$K_3Mo_{14}O_{22}$	$K_{1.66}Pb_{1.34}Mo_{14}O_{22}$	$K_{1.29}Sn_{1.71}Mo_{14}O_{22}$
Mo1–O1	2.01(1)	2.03(1)	2.009(7)
Mo1–O6	2.02(1)	2.03(1)	2.036(7)
Mo1–O10	2.11(1)	2.08(1)	2.097(7)
Mo1–O11′	2.10(1)	2.07(1)	2.058(8)
Mo2–O4	2.17(1)	2.13(1)	2.101(7)
Mo2–O5	2.04(1)	2.03(1)	2.011(7)
Mo2–O9	2.07(1)	2.07(1)	2.041(7)
Mo2–O10	2.12(1)	2.10(1)	2.113(7)
Mo2–O11	2.01(1)	2.03(1)	2.037(7)
Mo3–O2	2.12(1)	2.10(1)	2.086(7)
Mo3–O3	2.02(1)	1.97(1)	2.021(7)
Mo3–O6	2.00(1)	2.01(1)	2.038(7)
Mo3–O7	2.04(1)	2.03(1)	2.017(8)
Mo3–O8	1.95(1)	1.99(1)	2.061(7)
Mo4–O1	2.08(1)	2.05(1)	2.080(7)
Mo4–O5	2.04(1)	2.02(1)	2.048(7)
Mo4–O6	2.09(1)	2.10(1)	2.050(7)
Mo4–O7	2.09(1)	2.11(1)	2.064(7)
Mo4–O11	2.05(1)	2.05(1)	2.053(8)
Mo5–O3′	2.19(1)	2.17(1)	2.156(7)
Mo5–O4′	2.13(1)	2.14(1)	2.080(7)
Mo5–O8	1.92(1)	1.93(1)	1.963(7)
Mo5–O9′	2.00(1)	2.01(1)	2.029(8)
Mo5–O10	1.92(1)	1.93(1)	1.925(7)
Mo6–O1	2.04(1)	2.05(1)	2.015(7)
Mo6–O2	2.08(1)	2.07(1)	2.064(7)
Mo6–O5	2.09(1)	2.07(1)	2.060(7)
Mo6–O7′	2.01(1)	2.04(1)	2.041(7)
Mo7–O2	1.90(1)	1.98(1)	1.959(7)
Mo7′–O3′	1.97(1)	2.05(1)	1.981(7)
Mo7–O4	2.08(1)	2.10(1)	2.102(7)
Mo7–O4′	2.09(1)	2.11(1)	2.115(7)
Mo7–O9′	2.08(1)	2.10(1)	2.129(7)
Sn1A–O1[b]	na[c]	na	2.887(9)
Sn1A–O1′[b]	na	na	3.069(9)
Sn1A–O5[b]	na	na	2.38(1)
Sn1A–O5′[b]	na	na	3.23(1)
Sn1A–O6[b]	na	na	2.972(9)
Sn1A–O6′[b]	na	na	2.811(9)
Sn1A–O7[b]	na	na	2.42(1)
Sn1A–O7′[b]	na	na	3.10(1)
Sn1A–O11[b]	na	na	2.82(1)
Sn1A–O11′[b]	na	na	2.85(1)
K1–O1[b] (×2)	2.97(1)	2.93(1)	2.943(7)
K1–O5[b] (×2)	2.79(1)	2.77(1)	2.798(7)
K1–O6[b] (×2)	2.89(1)	2.88(1)	2.855(6)
K1–O7[b] (×2)	2.83(1)	2.78(1)	2.743(8)
K1–O11[b] (×2)	2.771(9)	2.72(1)	2.795(7)
M2–O2[b,d]	na	2.86(1)	3.020(7)
M2–O3[b,d]	na	2.75(1)	2.910(7)
M2–O4[b,d]	na	2.80(1)	2.936(7)
M2–O6[b,d]	na	2.91(1)	2.927(7)
M2–O8[b,d]	na	2.45(1)	2.215(6)
M2–O8′[b,d]	na	2.44(1)	2.272(7)
M2–O9[b,d]	na	2.56(1)	2.283(7)
M2–O10[b,d]	na	3.08(2)	3.072(7)
M2–O11[b,d]	na	2.85(1)	2.895(8)
K2A–O2[b,e]	2.96(1)	na	2.91(1)
K2A–O3[b,e]	2.80(1)	na	2.80(1)
K2A–O4[b,e]	2.94(1)	na	2.82(1)
K2A–O5[b,e]	3.05(1)	na	3.01(1)
K2A–O6[b,e]	2.95(1)	na	2.81(1)
K2A–O7[b,e]	3.13(1)	na	2.89(1)
K2A–O8[b,e]	2.71(1)	na	2.70(1)
K2A–O8′[b,e]	2.658(9)	na	2.76(1)
K2A–O9[b,e]	2.78(1)	na	2.76(1)
K2A–O10[b,e]	2.96(1)	na	2.95(1)
K2A–O11[b,e]	2.73(1)	na	2.77(1)

[a] Atoms with primed numbers are related to those with unprimed numbers by the inversion center. [b] Partially occupied positions in the K-Pb and K-Sn members. [c] na = not applicable. [d] M2 = K2/Pb2 in K-Pb member or Sn2 in the K-Sn member. [e] K2A = K2 in $K_3Mo_{14}O_{22}$.

Second, the interlinking of the cluster units along the chain also does not involve Mo3 in the intercluster bonding interactions, thus again leaving it free for stronger interactions with Mo5 and Mo7′. A more speculative thought is that the mixing of the apical $d_{x^2-y^2}$ orbitals with the same basal orbitals on the end Mo atoms, discussed by Wheeler and Hoffmann[26] for the Mo_{18} and Mo_{22} oligomers, is especially strong with the Mo_{14} members.

The average Mo−O bond distance for all three oligomeric members is 2.050 Å and is very similar to the 2.06 Å average distance reported for $Tl_{1.6}Sn_{1.2}Mo_{14}O_{22}$. The molybdenum−oxygen bond distances vary from 1.90(1) Å for Mo7−O2 to 2.19(1) Å for Mo5−O3′ in $K_3Mo_{14}O_{22}$, from 1.93(1) Å for Mo5−O10 to 2.17(1) Å for Mo5−O3′ in $K_{1.66}Pb_{1.34}Mo_{14}O_{22}$, and from 1.925(7) Å for Mo5−O10 to 2.156(7) Å for Mo5−O3′ in $K_{1.29}Sn_{1.71}Mo_{14}O_{22}$. All of these extreme bond distances occur in the region of intercluster bonding and can be rationalized from the coordination numbers of the molybdenums in question. The relatively short Mo−O bond distances are located at the ends of the trimer, where there is less metal−metal bonding, as compared to the interior molybdenums such as Mo1 and Mo6. The relatively long Mo−O bond distances are a result of direct involvement in the intercluster bonding. A complete listing of the metal−oxygen bond distances is given in Table 6.

Within the Mo_{14} cluster, four molybdenums are four-coordinate in oxygen (Mo1 and Mo6) and the remaining ten molybdenums are five-coordinate in oxygen (Mo2, Mo3, Mo4, Mo5, and Mo7). The connectivity of these $n = 3$ oligomers can be expressed by the following formulation, $[M_3]^{y+}[(Mo_{14}O^{i}{}_{10}O^{i\text{-}i}{}_{4/2}O^{i\text{-}a}{}_{10/2})O^{a\text{-}i}{}_{10/2}]^{y-}$, according to the labeling scheme proposed by Schäfer and von Schnering.[27] Oxygen atoms O5, O6, O7, O8, and O11 constitute the group labeled O^{i} and are edge-bridging within the cluster unit. O4 is defined as $O^{i\text{-}i}$ and is edge-sharing between neighboring clusters. Oxygen atoms labeled as $O^{i\text{-}a}$ and $O^{a\text{-}i}$ are edge-bridging between molybdenum atoms of one cluster and terminal to another molybdenum in a neighboring cluster (or vice versa); oxygen atoms O1, O2, O3, O9, and O10 define this class. The general features of this interconnectivity can be observed in Figures 2 and 3 for $K_{1.29}Sn_{1.71}Mo_{14}O_{22}$.

Cation Considerations. The voids in which the cations reside are not channels, but rather pockets in which both ends are partially closed by the neighboring Mo−O clusters. This pocket is formed as a result of the stair-step interconnection between clusters, as shown in Figure 3. The partial closure essentially traps the cations inside. From this arrangement of framework and cations, one could expect that the growth of these types of compounds is driven not only by the formation of a strongly metal−metal bonded framework, but also by the simultaneous formation of sites with suitable cation−oxygen interactions.

There are three cations per $Mo_{14}O_{22}$ cluster, with one cation position generally located adjacent to each Mo_6 octahedron, as illustrated in Figure 4 for $K_3Mo_{14}O_{22}$. The coordination around the potassium atoms in $K_3Mo_{14}O_{22}$ is shown in Figure 5a. K1 is located at the origin and adjacent to the central molybdenum octahedron of the trimer. It is surrounded by 10 oxygen atoms in a bicapped cubic geometry at distances ranging from 2.771(9) Å for K1−O11 to 2.97(1) Å for K1−O1. K2, located adjacent to the octahedra at either end of the clusters, is coordinated more irregularly by 11 oxygen atoms, with bond distances ranging from 2.658(9) Å for K2−O8′ to 3.13(1) Å for K2−O7. K1

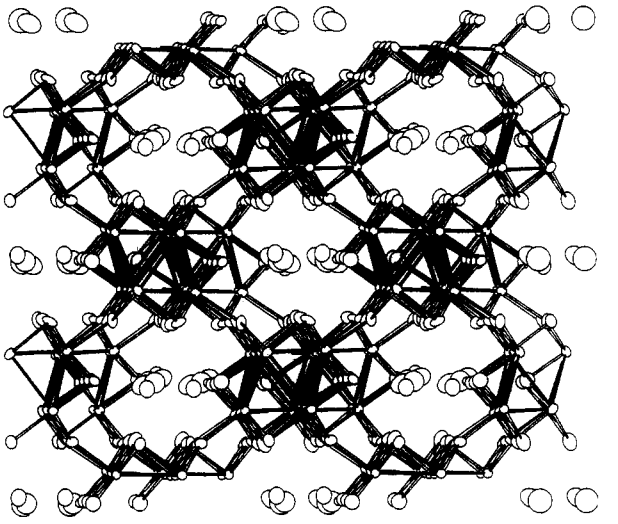

Figure 3. An ORTEP view (70% thermal ellipsoids) of $K_{1.29}Sn_{1.71}Mo_{14}O_{22}$ nearly parallel to the *c* axis. One adjacent set of trimeric cluster units is included in the *c* direction to indicate the nature of the cation pocket. Cation−oxygen bonds are omitted for clarity.

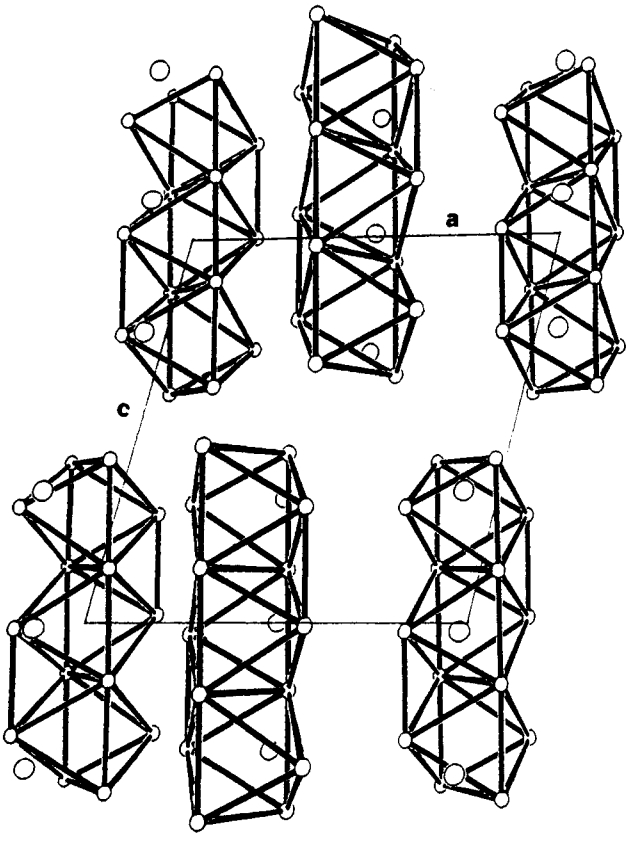

Figure 4. ORTEP drawing (50% thermal ellipsoids) of a perspective view of the condensed cluster units and potassium atoms in $K_3Mo_{14}O_{22}$ along [010]. Mo atoms are shown metal−metal bonded, oxygen atoms are omitted, and potassium atoms have larger thermal ellipsoids. Clusters are centered at $(0,{}^1/_2,0)$ and $({}^1/_2,0,0)$.

and K2 are separated by 3.181(3) Å within the pockets, a value that is almost exactly twice the ionic radius reported by Shannon for ten coordinate K^+.[28] The distance between two K2 atoms in adjacent pockets of neighboring Mo_{14} cluster units is 4.408(3) Å.

The coordination geometry of K1/Pb1 at the origin of $K_{1.66}Pb_{1.34}Mo_{14}O_{22}$ forms a bicapped cube, as shown in Figure 5b,

(26) Wheeler, R. A.; Hoffmann, R. *J. Am. Chem. Soc.* **1988**, *110*, 7315.
(27) Schäfer, H.; von Schnering, H. G. *Angew. Chem.* **1964**, *20*, 833.
(28) Shannon, R. D. *Acta Crystallogr.* **1976**, *A32*, 751.

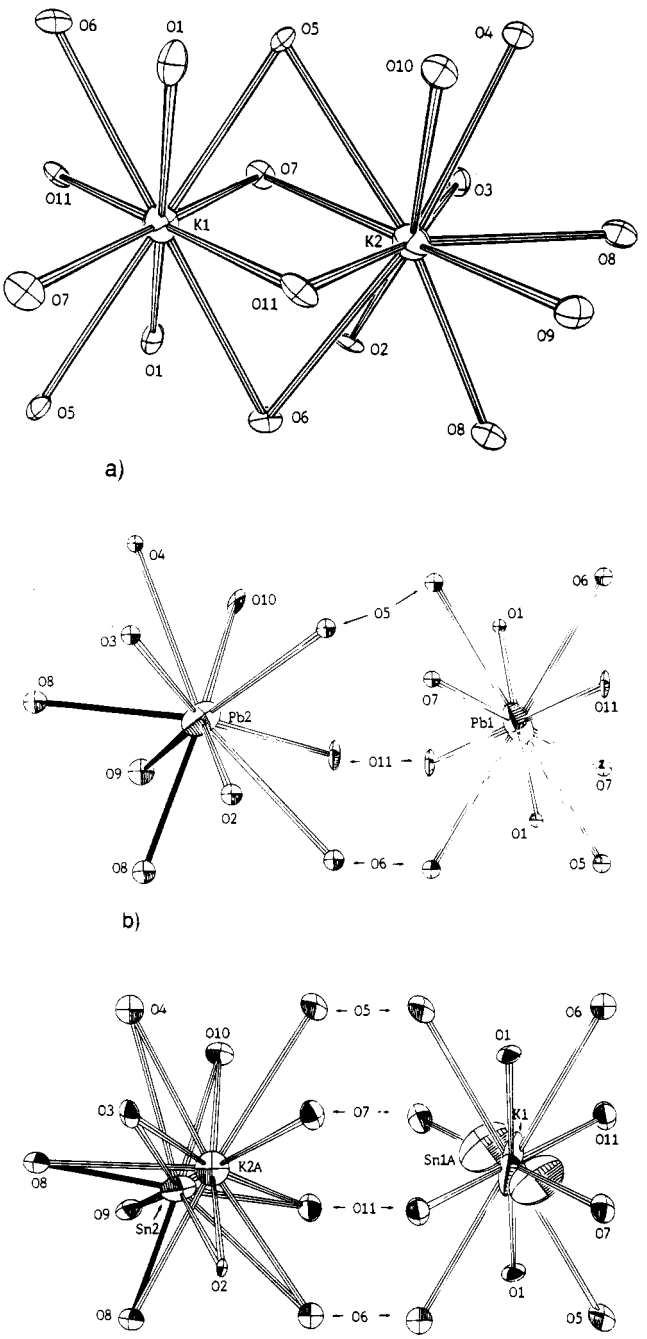

Figure 5. (a) Coordination of oxygen atoms around the potassiums in $K_3Mo_{14}O_{22}$. (b) Oxygen atom coordination around K1/Pb1 at the origin and the second cation site, Pb2/K2, in $K_{1.66}Pb_{1.34}Mo_{14}O_{22}$. The dark bonds represent short cation−oxygen bonds. (c) Oxygen atom coordination around the potassium at the origin and the tin satellites located on either side of the origin and the second major cation site, Sn2, and its satellite, K2A, in $K_{1.29}Sn_{1.71}Mo_{14}O_{22}$. The ORTEPs are drawn with 50% thermal ellipsoids for (a) and 70% thermal ellipsoids for (b) and (c).

with 10 oxygens ranging from 2.72(1) Å for K1/Pb1−O11 to 2.93(1) Å for K1/Pb1−O1. The other major cation site, Pb2/K2, is also 10-coordinate in oxygen and located adjacent to the end octahedra of the Mo_{14} unit. However, three of these oxygens are strongly bonded: Pb2/K2−O9 at 2.56(1) Å, Pb2/K2−O8 at 2.45(1) Å, and Pb2/K2−O8′ at 2.44(1) Å in a trigonal pyramidal geometry, and six more oxygens are weakly coordinated, ranging from 2.75(1) Å for Pb2/K2−O3 to 3.07(2) Å for Pb2/K2−O10. The coordination sphere also contains one very long (Pb2/K2−O7) distance at 3.21(1) Å. Unlike the cation situation to be described in $K_{1.29}Sn_{1.71}Mo_{14}O_{22}$, the mixed lead/potassium atoms occupy only three (two unique) positions within the cation pockets of $K_{1.66}Pb_{1.34}Mo_{14}O_{22}$. The cations are also well separated from each other, at 3.380(1) Å for Pb1−Pb2, and the interpocket Pb2−Pb2′ distance is even greater at 3.836(3) Å. Both distances are much longer than twice the ionic radii reported by Shannon[28] for 10-coordinate K^+ or Pb^{2+} (1.59 and 1.40 Å, respectively).

The compound $K_{1.29}Sn_{1.71}Mo_{14}O_{22}$ has seven partially occupied cation positions, four unique; however, the cations total three per formula unit. The arrangement in the K-Sn member is one in which the two major cation locations are similar to the K and K-Pb members. However, the combination of K and Sn results in a positionally disordered arrangement. The coordination for the K^+ at the origin for $K_{1.29}Sn_{1.71}Mo_{14}O_{22}$ is quite regular, as shown in Figure 5c, with 10 oxygens ranging from 2.743(8) Å for K1−O7 to 2.943(7) Å for K1−O1. The eight closest oxygens form a nearly regular cube around the potassium. The off-origin satellite Sn1A position has a coordination environment better suited to accommodate tin, based upon bond distances. This satellite tin position is irregular nine-coordinate in oxygen, with no definitive coordination geometry, ranging from 2.38(1) Å for Sn1A−O5 to 3.10(1) Å for Sn1A−O7′. This tin position (Sn1A) resides 0.464(9) Å on either side of the origin. The origin and its two satellites account for three of the seven positions. The other major cation site, Sn2, is nine-coordinate in oxygen; however, three of these oxygens are strongly bonded: Sn2−O9 at 2.283(7) Å, Sn2−O8 at 2.215(6) Å, and Sn2−O8′ at 2.272(7) Å. These three oxygens and the tin (Sn2) are arranged in a trigonal pyramidal geometry. The remaining six oxygens are weakly coordinated, ranging from 2.895(8) Å for Sn2−O11 to 2.936(7) Å for Sn2−O4. The satellite potassium atom, K2A, is located 0.660(8) Å from the major tin position, Sn2. K2A is 11-coordinate in oxygen, varying from 2.70(1) Å for K2A−O8 to 3.01(1) Å for K2A−O5. This second set of cation positions, plus their inversion related partners, account for the four remaining cation sites within one pocket. The seven cation positions occupied by potassium and tin in $K_{1.29}Sn_{1.71}Mo_{14}O_{22}$ are not aligned in a linear fashion, but rather their positions are skewed in such a manner as to create favorable coordination by oxygen atoms. This behavior can be seen in the cation angles, K1−Sn1A−K2A at 127.4(9)° and Sn1A−K2A−Sn2 at 153.(1)°. The cation arrangement is much more clear and simple in $K_3Mo_{14}O_{22}$ and $K_{1.66}Pb_{1.34}Mo_{14}O_{22}$. A complete listing of the cation−oxygen bond distances is given in Table 6.

The tendency of the cations in $K_{1.29}Sn_{1.71}Mo_{14}O_{22}$ to move off the "ideal" positions is probably promoted by the propensity of tin to exert its lone pair effect and obtain stronger interactions with a smaller number of oxygen atoms. These interactions are not suitable for a large cation such as potassium. The synthesis of such a quaternary phase, in which a hard cation, potassium, and a soft cation, tin, cooperatively mix, appears to result in multiple, partially occupied cation positions. Some of the cation−cation distances are shorter than the values predicted by use of Shannon radii.[28] However, the probability of occupying many of the combinations of satellite atom positions simultaneously is quite low; and from a chemical viewpoint, the possibility is highly unlikely because it would result in excessive cation−cation repulsions. The existence of a pure potassium oligomer, $K_3Mo_{14}O_{22}$, and a pure tin oligomer, $Sn_2Mo_{10}O_{16}$,[29] should lead one to expect that a mixed membered oligomer such as a $K_{1.29}Sn_{1.71}Mo_{14}O_{22}$ could be synthesized.

In contrast to the filled cation sites found here, $Tl_{1.6}Sn_{1.2}Mo_{14}O_{22}$ was found to contain cation vacancies, and some

(29) Gougeon, P.; Potel, M.; Sergent, M. *Acta Crystallogr.* **1990**, *C46*, 1188.

Table 7. Bond Length–Bond Strength Relationships and Electron Counting for the Trimeric Oligomers[a]

	$K_3Mo_{14}O_{22}$		$K_{1.66}Pb_{1.34}Mo_{14}O_{22}$		$K_{1.29}Sn_{1.71}Mo_{14}O_{22}$	
	Σn	Σs	Σn	Σs	Σn	Σs
Mo1	4.00(3)	2.34(8)	3.91(3)	2.38(7)	3.93(2)	2.41(5)
Mo2	3.12(2)	2.78(9)	3.35(2)	2.83(8)	2.94(1)	2.93(6)
Mo3	3.05(3)	3.3(1)	2.77(2)	3.30(9)	2.82(1)	3.05(6)
Mo4	3.31(3)	2.8(1)	3.34(3)	2.87(8)	3.18(1)	2.92(6)
Mo5	2.50(2)	3.35(8)	2.72(2)	3.28(9)	2.54(1)	3.28(7)
Mo6	3.96(3)	2.37(8)	3.80(3)	2.35(7)	3.91(2)	2.44(5)
Mo7	2.58(2)	3.3(1)	3.29(3)	2.88(9)	3.06(1)	3.01(6)
K1		1.15(3)		1.29(4)		1.23(2)
M1′				$1.74(3)^{Pb1}$		$1.64(3)^{Sn1A}$
M2		0.95(3)		$2.08(7)^{K2}$		$2.01(3)^{Sn2}$
M2′				$2.07(5)^{Pb2}$		$1.39(5)^{K2A}$
MCE[b]	45.0(4)	42.(1)	44.1(3)	44.(1)	42.7(2)	43.9(8)
formal[c]	43.0		44.3		44.7	

[a] Σn: Number of electrons available for Mo–Mo bonding within the cluster unit, based upon Pauling's bond order equation;[32] does not include intercluster bonds. Σs: Number of electrons available for Mo–Mo bonding within the cluster unit, derived from the Mo–O bond distance–bond valence sums.[35] For comparison: $Tl_{1.6}Sn_{1.2}Mo_{14}O_{22}$, MCE($\Sigma n$) = 43.4, MCE($\Sigma s$) = 45.5, formally 45.6, and individual Σs(Mo1 to Mo7, Tl1, Tl2, Sn) = 2.4, 2.9, 3.0, 2.9, 3.2, 2.4, 3.0, 1.7, 1.8, and 2.2, respectively.[12] [b] Total number of MCE: $2\Sigma(\Sigma(n \text{ or } s))$, see text. [c] Formal number of electrons available for Mo–Mo bonding, based upon six electrons from each Mo and the following oxidation states: Tl_2^{4+}, Sn^{2+}, Pb^{2+}, K^+, and O^{2-}.

cation–cation distances were sufficiently short to warrant the postulation of Tl_2^{4+} dimers.[12]

An interesting question arises as to whether or not there are extensive regions of intergrowth having different K^+/Sn^{2+} or K^+/Pb^{2+} ratios and if an ordering of the cations exists? It would appear to be highly likely, based upon the microprobe analyses and the ability of the Mo_{14} unit to accept a variety of electron counts, that variable compositions do exist and that a different crystal would have resulted in another composition. If the cations were ordered in some manner, a superstructure should be observed. Based upon previous work with superstructures generated by cation ordering,[30] TEM should give the best possibility for observing such phenomena. However, extensive selected area electron diffraction and high resolution imaging has not revealed any superstructuring effects in $K_{1.29}Sn_{1.71}Mo_{14}O_{22}$.[31]

Structure and Metal–Metal Bonding Considerations. The Pauling[32] type equation, $d(n) = 2.614 - 0.61 \log(n)$, has been used to calculate Mo–Mo bond order sums for many ternary reduced molybdenum oxides.[7,22,25] The results for the trimeric oligomers are given in Table 7. The pattern observed for the individual molybdenum atom bond order sums in selected oligomeric members, $Tl_{1.6}Sn_{1.2}Mo_{14}O_{22}$,[12] $In_6Mo_{22}O_{34}$,[13] $Ba_3Mo_{18}O_{28}$,[22] and $Pb_2Mo_{10}O_{16}$,[33] are also followed by the Mo atoms in $K_3Mo_{14}O_{22}$, $K_{1.66}Pb_{1.34}Mo_{14}O_{22}$, and $K_{1.29}Sn_{1.71}Mo_{14}O_{22}$. The interior molybdenum atoms in the basal plane have the greatest number of metal–metal bonds (Mo1 and Mo6) and, therefore, utilize the greatest number of MCE (metal cluster electrons). Molybdenum atoms with an intermediate number of metal–metal bonds (apical atoms Mo2, Mo3, and Mo4) contribute about one electron per molybdenum less than the former group. And molybdenum atoms located at the ends of the cluster (Mo5 and Mo7) have the fewest metal–metal bonds and consequently make available the least number of electrons for metal–metal bonding.

The number of MCE per formula unit reported at the bottom of Table 7 are obtained by summing the individual values over all the Mo atoms of the cluster unit. A comparison of these sums and the formal MCE count is in reasonable agreement for the K-Pb member; however, significant differences are observed for the K and K-Sn members. From a previous intensive study of Mo–Mo bond order sums,[25] the lower than expected number of MCE for the K-Sn oligomer can be attributed to some of the electrons available for metal–metal bonding entering non- or antibonding orbitals. For $K_3Mo_{14}O_{22}$, the larger than expected number of MCE is difficult to understand. In part, it might be attributed to the choice of $d(1)$, the Mo–Mo single bond distance,[22] which is not optimized for this type of compound.

The number of electrons formally available for metal–metal bonding is 43.0 in $K_3Mo_{14}O_{22}$, 44.3 in $K_{1.66}Pb_{1.34}Mo_{14}O_{22}$, and 44.7 in $K_{1.29}Sn_{1.71}Mo_{14}O_{22}$, given K^+, Sn^{2+}, Pb^{2+}, O^{2-}, and six electrons per molybdenum. These electron counts are all lower than that of Simon's previously reported $n = 3$ oligomer, $Tl_{1.6}Sn_{1.2}Mo_{14}O_{22}$[12] (45.6e). The variation of MCE in these trimeric cluster units correlates well with the apical–apical and intercluster molybdenum bond distances, and a few generalizations can be extracted. When only 43e are available for metal–metal bonding, as in $K_3Mo_{14}O_{22}$, the clusters are interconnected primarily by metal–oxygen bonding while two strong apical Mo–Mo interactions and the strong Mo3–Mo5 and Mo3–Mo7′ interactions maximize the electrons available. When the system accepts up to approximately one more electron, it appears to be utilized in orbitals for intercluster metal–metal bonding, and the apical–apical bonding remains strong, as observed in $K_{1.66}Pb_{1.34}Mo_{14}O_{22}$ bond distances. When the system contains between 44e and 46e, as in $K_{1.29}Sn_{1.71}Mo_{14}O_{22}$ and $Tl_{1.6}Sn_{1.2}Mo_{14}O_{22}$, the HOMO electrons must be entering nonbonding or, more likely, antibonding orbitals. The latter choice appears more reasonable since the apical Mo–Mo bond order sums total 1.35e for the K-Sn member versus 2.28e for the K-Pb member. Even though the K-Sn member formally has more electrons available for metal–metal bonding, the K-Pb member with its short–long apical Mo configuration utilizes the electrons more efficiently for metal–metal bonding. The intercluster bonding is also drastically weakened in $K_{1.29}Sn_{1.71}Mo_{14}O_{22}$ relative to the K-Pb member. If a material with greater than 46e for metal–metal bonding could be synthesized, the electrons would most certainly enter antibonding orbitals, and perhaps this observation is an indication of the upper limit above which no trimeric oligomer can be formed.

Metal–Oxygen Bond Length–Bond Strength Relationships. The implications of bond length–bond strength calculations for molybdenum oxides have also been well studied.[22,25,34] The empirical bond valence equation, $s(\text{cation-O}) = [R(\text{cation-O})/R(1)]^{-N}$, developed by Brown and Wu[35] was used here with values of $R(1)$ and (N), for Mo, K^+, Sn^{2+}, and Pb^{2+}, respectively, of 1.882 Å (6.0), 2.276 Å (9.1), 1.860 Å (4.5), and 2.044 Å (5.5). Based upon this equation, the bond valence sums were calculated for each of the molybdenum atoms and the cations, where for the latter only bond distances resulting in a net individual bond valence greater than 0.1 were included. These values are reported in Table 7. The MCE counts were derived from Mo–O bond valence sums by subtracting $2\Sigma(\Sigma s)$ from $(6 \times 14) = 84$, the maximum number of valence electrons

(30) Schimek, G. L.; McCarley, R. E.; Chumbley, L. S. *J. Mater. Res.* **1994**, *9*, 891.
(31) Ramlau, R.; Simon, A.; Schimek, G. L.; McCarley, R. E. *Z. Anorg. Allg. Chem.*, in press.
(32) Pauling, L. *The Nature of the Chemical Bond*, 3rd ed.; Cornell University Press: Ithaca, NY, 1960.
(33) Dronskowski, R.; Simon, A.; Mertin, W. *Z. Anorg. Allg. Chem.* **1991**, *602*, 49.
(34) Bart, J. C. J.; Ragaini, V. *Inorg. Chim. Acta* **1979**, *36*, 261.
(35) Brown, I. D.; Wu, K. K. *Acta Crystallogr.* **1976**, *B32*, 1957.

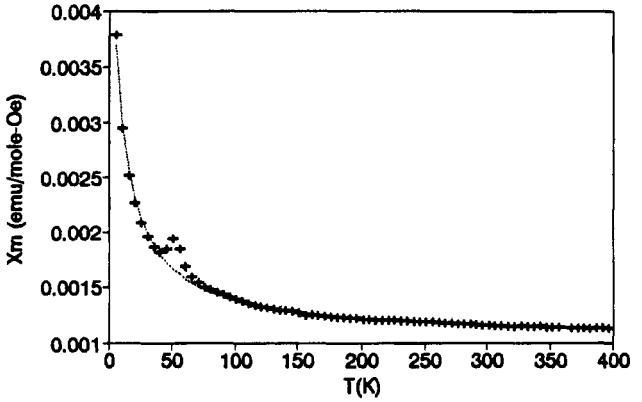

Figure 6. Molar magnetic susceptibility of $K_3Mo_{14}O_{22}$. The small anomaly at 50 K is an antiferromagnetic transition in adventitious adsorbed O_2. The dotted line represents the best least-squares fit to the Curie–Weiss expression.

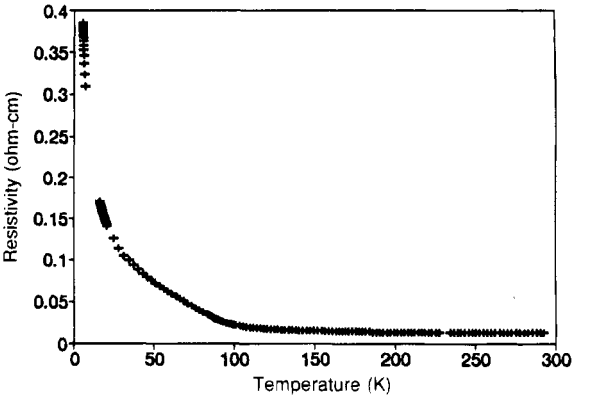

Figure 7. Resistivity versus temperature for a pressed, sintered pellet of $K_3Mo_{14}O_{22}$.

available from molybdenum. Within the estimated errors, the resulting values were in good agreement with the formal electron counts and with the description of the bonding given above.

In general, the bond valence sums calculated for potassium cations are too high, and the tin and lead cation valences are too low, especially when the cations reside on or near sites of partial occupation. This result is reasonable since the cation–oxygen distances utilized are averaged by the disorder in the cation positions. Therefore, bond valence sums do not necessarily work as well for the mixed member oligomeric cations. However, the values generally reflect the ability to distinguish between mono- and divalent cations.

Magnetic Properties. The molar magnetic susceptibility data of $K_3Mo_{14}O_{22}$, collected on a powdered sample over the temperature range of 5–400 K, are shown in Figure 6. All the data were corrected for diamagnetic core contributions, based upon the composition determined by microprobe analyses and the single crystal refinements, using values for individual ions reported by Selwood.[36] The data fit the equation $\chi_M^C = (C/T - \theta) + \chi_0 = (0.0367/T + 7.8) + 1.043 \times 10^{-3}$ emu/mol, from which an apparent moment of 0.54 μ_B per cluster unit is calculated. This apparent moment is too low for one unpaired electron per cluster unit, as might be expected for the odd electron count. This value is reproducible for samples from different preparations and could correspond to an electron trapped on one cluster out of every ten.

Dronskowski *et al.*[13] discuss increasing moments with increasing oligomer size based on the magnetic properties of four compounds having $n = 2-5$. However, the moment of $0.54\mu_\beta$ for $K_3Mo_{14}O_{22}$ is far lower than that of 1.2 μ_B for $Tl_{1.6}Sn_{1.2}Mo_{14}O_{22}$. This illustrates that the MCE and other factors may heavily influence the moment for a given cluster size. With the very limited number of compounds measured, we believe that a clear conclusion about the trend in moment vs oligomer size cannot be drawn.

It seems more likely that the low moment arises from a paramagnetic impurity. A third scenario is that the pure compound, $K_3Mo_{14}O_{22}$, might be spin-coupled between cluster units and result in diamagnetic behavior, even though the intercluster Mo–Mo bonding is weak. Another possibility is that the low susceptibility is associated with a charge disproportionation, forming clusters with 42 and 44 valence electrons. However, there are no known compounds in this series with 42 electron trimeric clusters to suggest the stability of such a unit.

(36) Selwood, P. W. *Magnetochemistry*, 2nd ed.; Interscience Publishers: New York, NY, 1956; p 78.

The magnetic susceptibility of $K_{1.66}Pb_{1.34}Mo_{14}O_{22}$ and $K_{1.29}Sn_{1.71}Mo_{14}O_{22}$ was measured on selected crystals over the temperature range of 6–356 K. Based upon microprobe analysis, there was variable composition for both members; thus their purity as line compounds is suspect. Therefore, the significance of the data is uncertain. In both compounds low moments derived from data below 50 K indicated the presence of paramagnetic impurities or effects like those discussed above for $K_3Mo_{14}O_{22}$. At temperatures above 150 K, only χ_{TIP} was shown by these materials, corresponding to 25 and 102 ($\times 10^{-6}$) emu/Mo for the K-Pb and K-Sn compounds, respectively.

Resistivity Investigations. Measurements of the electrical behavior of the $K_{1.66}Pb_{1.34}Mo_{14}O_{22}$ and $K_{1.29}Sn_{1.71}Mo_{14}O_{22}$ members were not undertaken because the cationic composition appeared to be quite variable based upon microprobe analyses. And thus, any results obtained would be suspect, especially since the variation on electron count has a dramatic effect on apical–apical and intercluster bonding. Figure 7 shows the pressed pellet resistivity data of $K_3Mo_{14}O_{22}$ in the temperature range of 5–297 K. The pressed pellet resistivity at room temperature is *ca.* 2.0×10^{-2} ohm·cm and falls in the window typical of a semiconductor. The resistivity from 100 to 297 K is nearly constant, but increases markedly below 100 K. This behavior is characteristic of a semiconductor, and the leveling off at higher temperatures suggests that the band gap is small. This behavior is also in agreement with that of $Tl_{1.6}Sn_{1.2}Mo_{14}O_{22}$ reported by Dronskowski, Mattausch, and Simon.[12] Except in the latter case, the resistivity did not level off to a constant value at higher temperatures. In these two cases, the resistivities behave contrary to the expectation from the shortest intercluster Mo–Mo distances. The K member with the larger intercluster distance apparently has the lower resistivity, 0.02 ohm·cm, compared to the Tl-Sn compound, 0.05 ohm·cm.

Conclusions

The three trimeric oligomers, $K_3Mo_{14}O_{22}$, $K_{1.66}Pb_{1.34}Mo_{14}O_{22}$, and $K_{1.29}Sn_{1.71}Mo_{14}O_{22}$, discussed here and the previously reported $Tl_{1.6}Sn_{1.2}Mo_{14}O_{22}$[12] begin to show the electronic flexibility that can be realized in finite chains of edge-shared molybdenum octahedra. In particular, the electron count available for metal–metal bonding has a significant impact on the magnitude of apical–apical and intercluster metal–metal bonding. The K, K-Pb, and K-Sn members all have Mo–O bond valence sums that correlate reasonably well with the electron count derived from the formal oxidation states. The Mo–Mo bond order sum for $K_3Mo_{14}O_{22}$ was larger than predicted and may be too high because of a slightly inappropriate value of $d(1)$, the Mo–Mo single bond distance. Also, the Mo–

Mo bond order sum did not fit the formal electron count for $K_{1.29}Sn_{1.71}Mo_{14}O_{22}$, in contrast to that for $K_{1.66}Pb_{1.34}Mo_{14}O_{22}$, which was close to the expected value. This discrepancy is most likely the result of electrons entering non- or antibonding states in the K-Sn member, while all the electrons available for metal−metal bonding are utilized as such in the K or K-Pb members. The nearly equivalent apical−apical bonds and relatively long intercluster interaction in $K_{1.29}Sn_{1.71}Mo_{14}O_{22}$ are similar to those of $Tl_{1.6}Sn_{1.2}Mo_{14}O_{22}$. The $K_3Mo_{14}O_{22}$ and $K_{1.66}Pb_{1.34}Mo_{14}O_{22}$ members constitute two new arrangements, with short and long apical−apical molybdenum bond distances formed by a sliding motion of the apical atoms. There is also a significant intercluster metal−metal bond for the K-Pb member. The magnetic properties of the K, K-Pb, and K-Sn members are not easily interpreted with respect to their formal electron counts. The low effective moments for $K_3Mo_{14}O_{22}$ and $K_{1.29}Sn_{1.71}Mo_{14}O_{22}$, if not due to impurities, require further work for clarification.

Acknowledgment. We would like to thank Dr. Robert A. Jacobson for guidance during the utilization of his crystallographic programs. Assistance with the magnetic susceptibility was provided by Jerry Ostenson. The microprobe analyses were completed by Dr. Alfred Kracher, Department of Geological and Atmospheric Sciences, at Iowa State University. This work was supported by the U.S. Department of Energy, Office of Basic Energy Sciences, through Ames Laboratory operated by Iowa State University under Contract W-7405-Eng-82.

Supporting Information Available: Tables listing the anisotropic thermal parameters and selected bond angle information (6 pages). Ordering information is given on any current masthead page.

IC950891P